Journal of Alzheimer's Disease 60 (2017) 439–450
DOI 10.3233/JAD-170390
IOS Press

PET Imaging of Tau Pathology and Relationship to Amyloid, Longitudinal MRI, and Cognitive Change in Down Syndrome: Results from the Down Syndrome Biomarker Initiative (DSBI)

Michael S. Rafii[a,b,*], Ana S. Lukic[c], Randolph D. Andrews[c], James Brewer[b], Robert A. Rissman[b,g], Stephen C. Strother[c,d], Miles N. Wernick[c,e], Craig Pennington[c], William C. Mobley[b], Seth Ness[f] and Dawn C. Matthews[c] for the Down Syndrome Biomarker Initiative and the Alzheimer's Disease Neuroimaging Initiative[1]

[a]*Alzheimer's Therapeutic Research Institute (ATRI), Keck School of Medicine, University of Southern California, San Diego, USA*
[b]*Department of Neurosciences, University of California San Diego School of Medicine, La Jolla, CA, USA*
[c]*ADM Diagnostics, Northbrook, IL, USA*
[d]*Rotman Research Institute, Baycrest, Toronto, ON, CA, USA*
[e]*Medical Imaging Research Center, Illinois Institute of Technology, Chicago, IL, USA*
[f]*Janssen Research and Development LLC, Raritan, NJ, USA*
[g]*Veterans Administration Medical Center, La Jolla, CA, USA*

Handling Associate Editor: Sid O'Bryant

Accepted 7 July 2017

Abstract.
Background: Adults with Down syndrome (DS) represent an enriched population for the development of Alzheimer's disease (AD), which could aid the study of therapeutic interventions, and in turn, could benefit from discoveries made in other AD populations.
Objectives: 1) Understand the relationship between tau pathology and age, amyloid deposition, neurodegeneration (MRI and FDG PET), and cognitive and functional performance; 2) detect and differentiate AD-specific changes from DS-specific brain changes in longitudinal MRI.
Methods: Twelve non-demented adults, ages 30 to 60, with DS were enrolled in the Down Syndrome Biomarker Initiative (DSBI), a 3-year, observational, cohort study to demonstrate the feasibility of conducting AD intervention/prevention trials in adults with DS. We collected imaging data with ^{18}F-AV-1451 tau PET, AV-45 amyloid PET, FDG PET, and volumetric MRI, as well as cognitive and functional measures and additional laboratory measures.

[1]Data used in preparation of this article were obtained from the Alzheimer's Disease Neuroimaging Initiative (ADNI) database (http://adni.loni.usc.edu). As such, the investigators within the ADNI contributed to the design and implementation of ADNI and/or provided data but did not participate in analysis or writing of this report. A complete listing of ADNI investigators can be found at: http://adni.loni.usc.edu/wp-content/uploads/how_to_apply/ADNI_Acknowledgement_List.pdf.

*Correspondence to: Michael S. Rafii, MD, PhD, Alzheimer's Therapeutic Research Institute (ATRI), Keck School of Medicine, University of Southern California, 9860 Mesa Rim Road, San Diego, CA 92121, USA. Tel.: +1 858 964 0638; E-mail: mrafii@usc.edu.

ISSN 1387-2877/17/$35.00

Results: All amyloid negative subjects imaged were tau-negative. Among the amyloid positive subjects, three had tau in regions associated with Braak stage VI, two at stage V, and one at stage II. Amyloid and tau burden correlated with age. The MRI analysis produced two distinct volumetric patterns. The first differentiated DS from normal (NL) and AD, did not correlate with age or amyloid, and was longitudinally stable. The second pattern reflected AD-like atrophy and differentiated NL from AD. Tau PET and MRI atrophy correlated with several cognitive and functional measures.
Conclusions: Tau accumulation is associated with amyloid positivity and age, as well as with progressive neurodegeneration measurable using FDG and MRI. Tau correlates with cognitive decline, as do AD-specific hypometabolism and atrophy.

Keywords: Alzheimer's disease, biomarkers, dementia, Down syndrome, Tau PET, volumetric MRI

INTRODUCTION

Nearly all adults with Down syndrome (DS) develop amyloid plaques and neurofibrillary tangles consistent with Alzheimer's disease (AD) pathology as they reach their forties [1, 2]. Autopsy studies have shown that progression of neurofibrillary tangles in adults with DS follows a similar Braak staging as found in AD, initiating in the transentorhinal cortex, and then spreading to the hippocampus (Stage II), inferior temporal cortex, and neocortex [3]. Expansion beyond Stage II appears to be preceded by amyloid plaque accumulation, as is observed in AD patients without DS [2]. Consistent with pathology, AD-like dementia is observed in up to 55% of adults with DS in their forties and 77% in their sixties [1]. These similarities suggest that adults with DS may provide a naturally enriched population in which to evaluate AD-targeted therapeutics, and, in turn, could benefit from discoveries made in other AD populations [4].

To study the feasibility of conducting AD clinical trials in the DS population, a three-year DS Biomarker Initiative (DSBI) study was initiated by Janssen Research and Development in collaboration with the Adult Down Syndrome Program at the University of California San Diego (UCSD). This study was designed to demonstrate methodology feasibility for a larger natural history trial [5, 6]. Endpoints include neuropsychological testing, positron emission tomography (PET) imaging of cerebral amyloid with the radiotracer ^{18}F-AV-45 and glucose metabolism (FDG PET) at baseline, magnetic resonance imaging (MRI) at baseline, year 1, and year 2, blood biomarkers [5], and tau PET imaging at year 2 with the radiotracer ^{18}F-AV-1451. We previously reported our findings for baseline FDG PET, amyloid PET, and MRI [6], and now report results regarding tau PET and longitudinal MRI.

The PET tracer ^{18}F-AV-1451 has been shown to bind strongly and preferentially to neurofibrillary tangles, and most strongly to 3R + 4R tau, as found in AD as compared to other neurodegenerative diseases [7–9]. Its detection in adults with DS could provide further confirmation that their pathology is representative of typical AD. This also represents the first study of PET imaging in adults with DS using a tau-specific radiotracer. Prior studies have been based upon autopsy [2] or imaging with FDDNP PET, which measures combined amyloid and tau [10].

In this work, we investigated the regional distribution of tau and examined associations with amyloid burden, cognitive measures, and neurodegeneration measured using MRI and FDG. We also assessed longitudinal volumetric brain changes and associations with amyloid, tau, FDG, and cognitive endpoints. The cognitive measures included the Observer Memory Questionnaire (OMQ-PF), Vineland-II Adaptive Behavior Scale (VABS-II), the Cambridge Cognitive Examination (CAMCOG), and Repeatable Battery for the Assessment of Neuropsychological Status (RBANS) Total Score, as previously described [5]. The cognitive batteries were administered by a certified neuropsychologist with experience in testing adults with developmental disabilities. In our previous baseline analysis, using a novel machine learning approach (NPAIRS) [11, 12], we had identified two distinct patterns of volumetric differences within DS subjects. The first pattern differentiated DS from non-adults with DS with or without AD. The second pattern reflected an AD-like atrophy pattern, observed in the amyloid positive (Am+) DS subjects in varying degrees but not the amyloid negative (Am-) adults with DS [6]. We hypothesized that the DS-related pattern of atrophy would not progress longitudinally, whereas the AD-related pattern might progress in Am+ subjects who were experiencing neurodegeneration, with possible correlation to cognition. Of course, some brain structures may be affected by both DS characteristics and neurodegenerative processes.

METHODS

Subject selection

Twelve non-demented adults diagnosed with DS, age 30–60 y, were enrolled in DSBI, with subject inclusion and exclusion criteria described previously [5]. Nine had tau PET scans available and 10 had longitudinal MRI (of whom 8 had tau imaging). Of the 9 subjects imaged with tau PET, 7 were female; 4 were APOE ε4 carriers, and age range at tau scan was 32 to 62 y. Of the 10 subjects having longitudinal MRI, 8 were female, 5 were APOE ε4 carriers, and age at year 2 scan was 34 to 64 y. Assessments for enrollment were conducted by UCSD under IRB-approved protocols with patient informed consent.

Image data acquisition, processing, and analysis

Tau PET scans were acquired on a Siemens ECAT HR+ scanner from 75 to 105 min post tracer injection in six 5 min frames, using 10 mCi (370 MBq) of ^{18}F-AV-1451. MRI scans were acquired on a 1.5 Tesla GE Signa HDxt scanner using a series modeled on the non-accelerated T1-weighted sequence from ADNI. Tau PET images and longitudinal MRI scans were co-registered to the baseline MRI for each subject, which was spatially transformed to a common template using the DARTEL algorithm [13] in the VBM8 toolbox of SPM8 (Wellcome Trust). The transform was applied to the PET scans, which were smoothed using a Gaussian filter kernel of $5 \times 5 \times 5$ mm. The gray modulated segments produced by DARTEL were smoothed using an 8 mm Gaussian kernel for group analyses.

To evaluate distribution and extent of tau burden, region of interest (ROI) masks representing each successive Braak stage were developed using combinations of the relevant anatomical structures derived by Freesurfer on a template MRI (Fig. 1) based upon recent literature [14].

Reference regions for Standardized Uptake Value Ratio (SUVR) calculation were defined as cerebellar cortex (excluding bottom slices and eroded from edges) and for comparison, subcortical white matter (eroded from gray). Regional signal intensities were measured using PMOD version 3.3 (PMOD Technologies) and an overall Tau Braak score generated using the average of individual Braak stage values. Although this sample was too small to derive

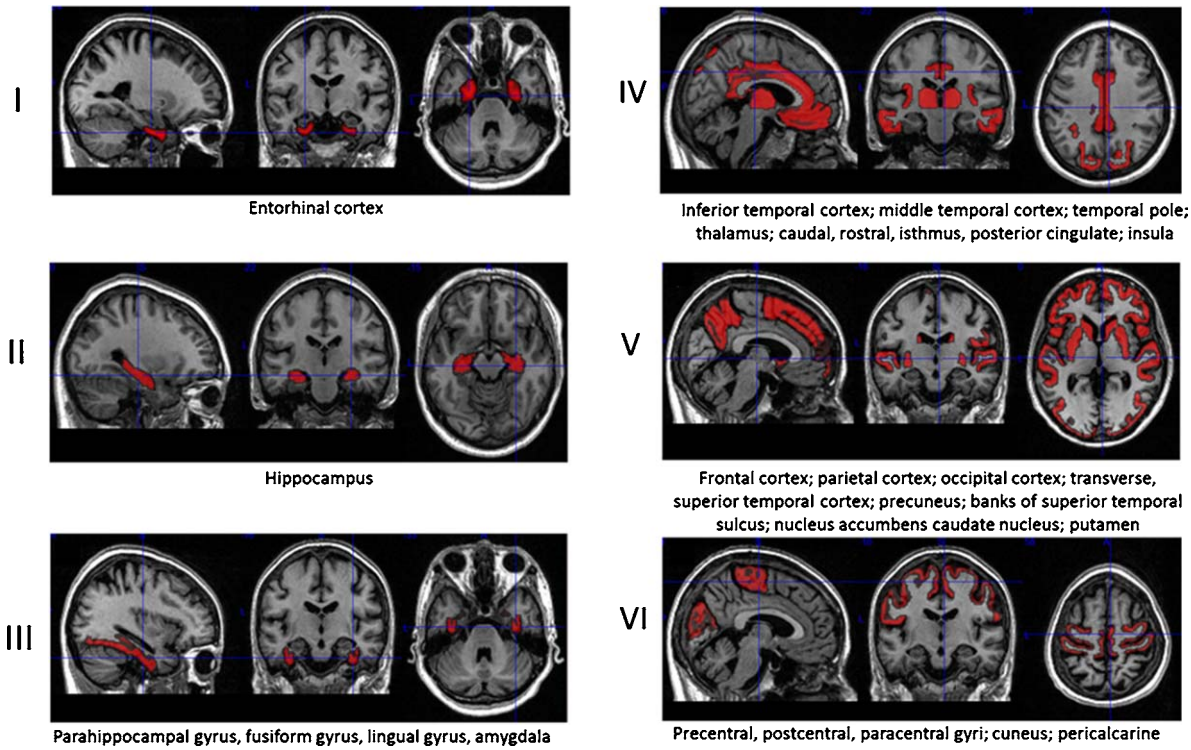

Fig. 1. Braak stage regions of interest (based upon Freesurfer ROIs listed at: https://jagustlab.neuro.berkeley.edu/).

a statistical cutoff for positivity, values within Am- subjects (mean of all Braak regions 1.02, SD 0.06) compared to those in Am+ subjects suggested a threshold of 1.2 (cerebellar reference) or 1.05 (white tissue reference). Values of 1.20 to 1.25 (cerebellar reference) were considered threshold positive. This threshold compared to a derived mean of approximately 1.08 for healthy controls of similar age based upon young and elderly values reported by Schöll et al. [14] and the identification of 1.2 as a threshold for elevated neocortical tau by Sperling [15], based upon data acquired in the A4 secondary prevention trial. Although the sample size was small and subject motion precluded segmentation in one individual, partial volume effects (PVE) correction was applied using the Muller-Gartner method [16] to some subjects as a comparator to uncorrected results, particularly to examine the hippocampus.

MRI analyses

NPAIRS multivariate analysis software [11, 12] was applied to the images to detect patterns that might characterize AD progression distinct from DS related effects. NPAIRS applies machine learning with intensive split half (50/50) resampling to identify stable, generalizable patterns that characterize similarities and differences between classes (groups) of images. Principal Component Analysis and subsequent Canonical Variates Analysis (a form of linear discriminant analysis) are employed to identify uncorrelated spatial patterns that when mathematically combined account for overall variance across groups. NPAIRS iteratively divides the data set into split halves many times, generating metrics of reproducibility (correlation between the model generated by each split half) and prediction (correct classification of the test half using the training half model) that are used to select parameters providing an optimal combination of reproducibility and prediction. A Canonical Variate (CV) score quantifies the degree to which each subject expresses each pattern. This approach addresses the issue of over-fitting that can arise in machine learning, particularly when data sets are small. The test (rather than training) scores were used to report results.

For comparison to DS subjects, two sets of 12 subjects were identified from the ADNI database based on ADNI clinical diagnosis, amyloid status, and age: Am- normal (NL), and Am+ AD. ADNI was launched in 2003 as a public-private partnership to test whether MRI, PET, other biological markers, and clinical and neuropsychological assessment can be combined to measure the progression of MCI and early AD (www.adni-info.org). The n of 12 was selected for balance across groups. Subjects were considered Am- if their cortical average SUVR was below 1.47 for ^{11}C-PiB [17] or <1.11 for florbetapir [18] or their cerebrospinal fluid (CSF) $A\beta_{42}$ was >209, and were considered Am+ if their amyloid PET SUVR exceeded threshold or their CSF $A\beta_{42}$ level was <192 [19]. Given the relatively young DS subject ages, the youngest ADNI subjects meeting diagnostic and amyloid criteria were selected. The feasibility of comparing these groups despite age, site, and scanner differences was demonstrated during our baseline analyses [6].

Statistical analyses

Each NPAIRS analysis generated measures of reproducibility and predictive power indicating whether results were generalizable. Group CV scores were evaluated for normality and homogeneity of variance, compared using non-parametric tests (Wilcoxon-Mann-Whitney) as the group sample sizes were 12 or less, and effect sizes (ES) were calculated (G*Power) [20].

Correlation coefficients (Spearman's r) were measured for tau Braak stage scores and structural MRI (sMRI) CV scores versus age, amyloid SUVR, and clinical measures. A p-value of 0.05 was considered significant with the caveat that due to the small sample size, these are included only as indicators of potentially significant relationships. Correction for multiple comparisons would reduce the significance threshold to 0.005 but this was not evaluated given the exploratory sample size.

RESULTS

Subject demographics and DS participant clinical scores are shown in Table 1.

Tau results: Tau burden and distribution

Figure 2 illustrates the tau (abnormally aggregated) distributions for individual Am- or threshold subjects (Fig. 2a) and Am+ subjects (Fig. 2b). SUVRs calculated using the cerebellar cortex reference are listed in Table 2. Tau burdens across subjects were similar for the two reference regions except DP09 whose cerebellum showed higher signal that in turn reduced Braak stage SUVR values.

Table 1
Subject characteristics

	DS	NL	AD
Number	12	12	12
Age (Mean (S.D.))	45 (8.5)	63 (2.5)	58 (2.5)
Gender (%F)	83%	67%	58%
Education (y)	13 (5.1)	17 (2.0)	16 (2.7)
APOE ε4 carrier %	50%	17%	67%
Amyloid positive	58%*	0%	100%
Individual DS participant characteristics			
Subject	*Age at baseline (y)*	*APOE ε4*	*Amyloid PET clinical read*
DP01	32	E3-E3	Negative
DP07	34	E2-E4	Negative
DP06	37	E3-E3	Negative
DP08	39	E3-E3	Positive*
DP02	45	E2-E3	Positive
DP12	45	E3-E4	Positive
DP11	47	E3-E4	Positive
DP05	48	E3-E3	Positive
DP13	50	E3-E4	Positive
DP03	52	E3-E4	Positive
DP04	55	E3-E4	Positive
DP09	60	E3-E3	Positive

*DP08 had a threshold (borderline negative) amyloid SUVR when quantitatively measured. Other subjects had agreement between clinical (visual) and quantitative reads.

We observed that the anatomic localization for ^{18}F-1451 binding in adults with DS was similar to that which has been reported in individuals with AD, including medial temporal, inferolateral temporal, precuneus, and posterior cingulate regions. Five of the six tau positive subjects followed sequential Braak staging, whereby all stages below the highest positive stage were also positive. One subject exhibited hippocampal sparing, even when white matter tissue reference was used instead of the cerebellum, and with or without PVE correction.

Tau positive subjects exhibited patterns similar to the progressive glucose hypometabolism observed in typical AD [21, 22]. Patterns in four subjects were quite symmetrical whereas one subject had asymmetry and greater occipital deposition relative to other regions.

All subjects had PET signal in regions termed "off target" in the literature, including sphenoid bone/sinus, melanin containing tissue surrounding the eyes, globus pallidus, and dura [8].

Relationship of tau to amyloid burden

No tau accumulation in Braak stage regions was observed in Am- or threshold subjects, whereas Am+ subjects exhibited a range of Braak stage binding ranging from II to VI. As shown in Fig. 3, Tau Braak scores correlate (Spearman's r, two-tailed p) with subject age ($r = 0.75$, $p < 0.019$) and cortical average amyloid SUVR ($r = 0.79$, $p < 0.012$). Subject DP09 was no longer an outlier when tau intensities were normalized to the white tissue reference, and Tau Braak scores correlate with age ($r = 0.73$, $p < 0.025$) and amyloid status ($r = 0.80$, $p < 0.010$).

Tau correlation to cognitive endpoints

Consistent with the hypothesis that tau deposition is detrimental to cognition and function, as previously reported in AD [23], those with greater ^{18}F-AV-1451 binding had lower scores on baseline tests of cognition and function. Figure 4 shows the correlation (Spearman's r, two-tailed p) between Tau Braak stage value with OMP-QF [24] ($r = –0.59$, $p < 0.09$ at baseline, $r = –0.78$, $p < 0.02$ at 2 y), and with baseline VABS-II Daily Living Skills ($r = –0.76$, $p < 0.02$), CAMCOG Recent Memory ($r = –0.61$, $p < 0.08$), VABS-II composite ($r = –0.70$, $p < 0.03$), Socialization skills ($r = –0.90$, $p < 0.001$), and RBANS Total Score ($r = –0.74$, $p < 0.02$). Am- subjects had highest (least dysfunctional) values. Although age could not be dissociated from disease-related pathology in this small set, the associations exceeded those due to age alone in non-AD populations.

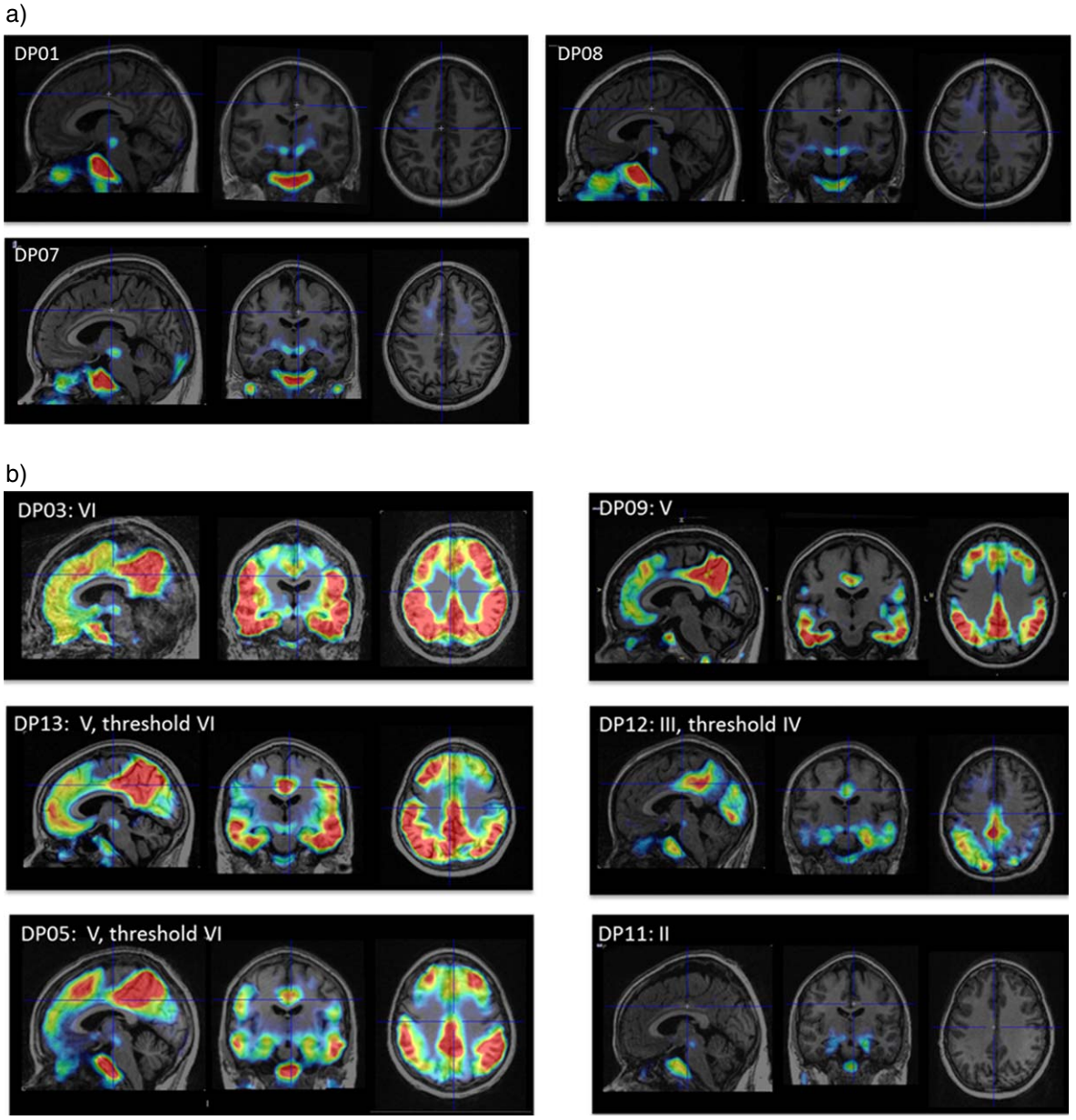

Fig. 2. (a) Tau distribution in subjects who were amyloid negative or at threshold on amyloid PET. (b) Tau distribution in subjects who were positive on amyloid PET. Subjects are thresholded to cerebellar cortex and the same display thresholds applied across all subjects with the exception of subject DP09, whose reference was adjusted using a white matter correction due to the observation of high signal intensities in cerebellum. In that case, the pattern of regional positivity was the same but values were greater and at least stage V, while hippocampal values were still tau negative.

Structural MRI results

Canonical variate patterns

Nine subjects having longitudinal MRI were included in the NPAIRS analysis; one subject (DP03) was excluded due to motion.

Figure 5 presents results from the 3-class NPAIRS analysis of modulated gray MRI segments of DS, NL, and AD, which produced two CVs. The first CV (Fig. 5a, $CV1_{sMRI}$) differentiated DS from NL ($p < 0.00001$, ES 3.94 at baseline) and AD ($p < 0.00001$, ES 4.87 at baseline) (Wilcoxon-Mann-

Table 2
Braak stage Standardized Uptake Value Ratios normalized to gray cerebellum

SUVR in each incremental Braak stage region (gray = tau positive)									
Braak stage ROIs	Amyloid negative or threshold participants			Amyloid positive participants					
	DP01	DP07	DP08	DP11	DP12	DP05	DP13	DP03	DP09
1	1.00	1.14	1.05	1.35	1.64	1.60	1.48	1.99	1.36
II	1.03	1.11	1.05	1.41	1.54	1.59	1.33	2.36	1.01
III	1.02	1.07	1.04	1.10	1.43	1.47	1.84	1.60	1.39
IV	1.01	1.05	0.96	1.04	1.23	1.57	1.63	1.94	1.28
V	0.99	1.02	0.95	0.97	1.11	1.56	1.52	2.17	1.24
VI	0.94	0.95	0.92	0.88	0.90	1.21	1.10	1.92	0.93

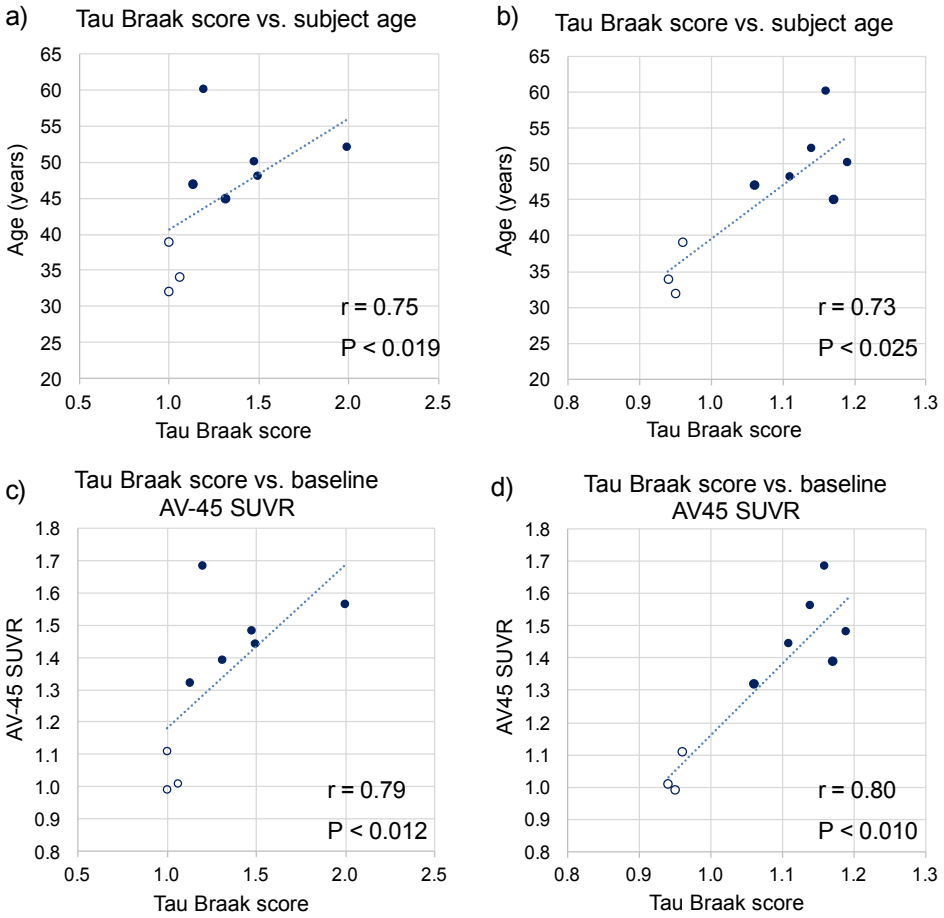

Fig. 3. Relationship between Tau Braak score and subject age using (a) cerebellar cortex reference and (b) white tissue reference, and AV-45 SUVR using (c) cerebellar cortex reference and (d) white tissue reference.

Whitney *t*-tests). Consistent with our previous results and the literature [25, 26] and relative to NL and AD, this pattern reflects volumetric reductions in cerebellum, occipital cortex, hippocampus, mid-cingulate, anterior cingulate, and temporal cortex, while preserved or increased volume is seen in caudate, putamen, thalamus, inferior lateral temporal, inferior parietal, and prefrontal cortices. There is no association between $CV1_{sMRI}$ score and amyloid status or age in DS subjects. This pattern was stable in DS subjects longitudinally, as shown in the Fig. 5a CV1 plot. The second pattern, $CV2_{sMRI}$ (Fig. 5b), differentiated NL from AD ($p < 0.00001$, ES 2.26), whereas DS scores distributed across the range from NL to AD as in our previous analysis of baseline data. This pattern showed volume reductions in posterior

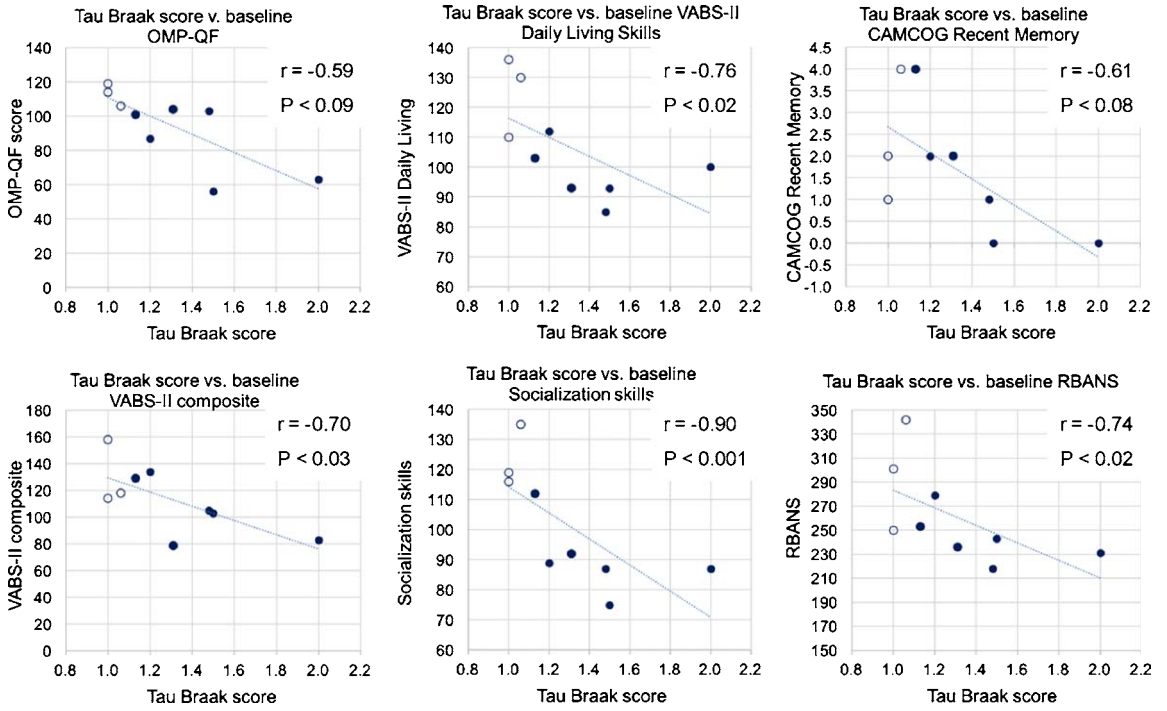

Fig. 4. Relationship between Tau Braak score (cerebellar cortex reference region) and OMP-QF, VABS-II Daily Living Skills, CAMCOG Recent Memory, VABS-II composite, Socialization skills, and RBANS Total Score at baseline.

cingulate, precuneus, parietal cortex, hippocampus, temporal cortex, frontal cortex, and caudate, with preserved or increased volume in putamen, thalamus, and midbrain. Volume reductions were consistent with AD atrophy [27, 28]. Four of five subjects with the lowest $CV2_{sMRI}$ scores were Am- or threshold, while the fifth was Am+ but only tau Braak stage II. Despite correlation with age in DS subjects, this pattern was not age-related in non-DS subjects, suggesting association with disease progression.

Longitudinal change in CV2 scores as related to tau burden and clinical measures

Am- subjects and the tau Braak stage II subject showed little or no longitudinal increase in score. Subjects who were Am+ and Braak stage IV or greater showed varying degrees of longitudinal progression, which increased with baseline score. The greatest baseline score and subsequent increase were exhibited by an Am+ 45-year-old subject without tau imaging, but whose Daily Living scores declined by 58 points, the largest decline among subjects, and whose VABS-II Adaptive Behavior composite decreased by 50 points over the 2 years, the second largest decline of subjects having longitudinal MRI. The second greatest increase in CV2 score, and greatest score at baseline, were those of a subject with highest tau score (white matter reference) of those having longitudinal MRI, and whose Daily Living score decreased by 36 points, and OMP-QF by 15 points. By comparison, the subjects having baseline CV2 scores near zero with little or no longitudinal increase were similar to one another in tau score, and showed less worsening (–14), or else improvement, in Daily Living Scores. The tau Braak stage II subject, who did not increase in MRI score, improved in Daily Living score. There was no observed decline on the other measures of cognition in the Am- group.

Tau correspondence with FDG PET

Within subjects, tau PET at year 2 and FDG PET at baseline showed certain regional similarities, with some differences, after dissociating DS-related effects. In general, areas of hypometabolism as seen with ^{18}F-FDG PET is consistent with areas of tau accumulation as seen with ^{18}F-AV-1451 (Fig. 6).

DISCUSSION

In this small and preliminary study, we have demonstrated for the first time the measurement of tau

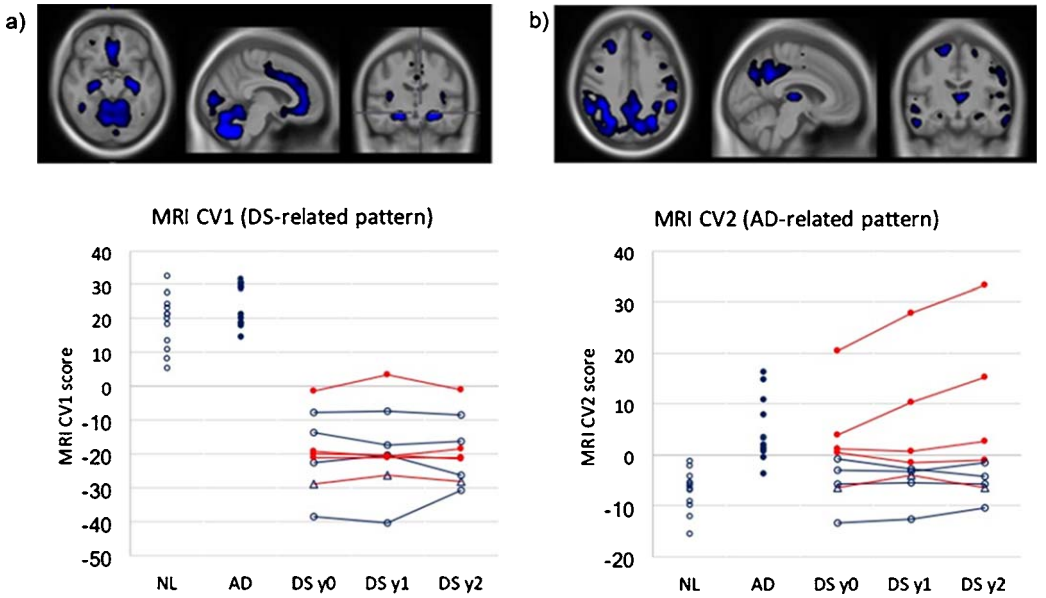

Fig. 5. (a) The CV1 pattern of volumetric reduction in DS subjects relative to NL or AD subjects, and the corresponding CV1 score plot. (b) The CV2 pattern of AD-like atrophy in AD subjects and certain Am+ DS subjects relative to NLs. Circles represent classifier scores for each subject, whereby a higher score indicates greater pattern expression relative to subjects with low scores. Unfilled dark blue circles with blue lines are subjects who were Am-, and filled red circles with red lines are Am+ Tau+ subjects. The unfilled triangle with red lines represents the Am+ subject with tau at Braak stage II.

pathology accumulation in adults with DS using the PET tracer ^{18}F-AV-1451, and its relationship to amyloid burden, regional cerebral glucose metabolism, brain volume, and cognitive and functional status. As seen in the non-DS population with prodromal AD or AD dementia, tau distribution is generally concordant with the neurodegenerative pattern reflected by FDG PET and structural MRI, involving the medial temporal cortices and spreading posteriorly and dorsally into the parietal cortices. Spatial overlap between tau distribution and neurodegeneration has been noted in other dementias [29]. Differences found may be due to downstream effects of tau pathology upon function in cases where FDG hypometabolism exceeded tau, signal effect size differences, or lag in neuronal damage. Regional variability was also observed as with both tau PET and FDG in AD patients [30]. The "off target" tau binding observed in the majority of DS subjects, whether or not Am+ was consistent with findings in other populations [8]. It remains unclear which isoforms of striatal tau we are detecting with ^{18}F-AV-1451 binding. Of note, different amyloid and tau species have been reported neuropathologically based on immunostaining techniques and this is likely true with PET tracers.

One Stage V subject was notable for relative absence of tau in hippocampus, even after PVE correction. Hippocampal sparing has been noted in other studies of AD subjects, leading to suggested sub-classifications as hippocampal sparing versus limbic predominant [30]. Additional subjects are necessary to explore subclass implications. The same subject had high signal intensities in cerebellar cortex, which could have arisen from technical confounds but appeared to be tracer binding. Tau accumulation in cerebellum has been noted in some early onset AD subjects [31].

The relationship between tau burden and amyloid SUVR is consistent with that noted in late onset AD, where it has been noted that the presence of tau beyond medial temporal regions appears predicated upon amyloid positivity [14]. A larger population may show that the correlation between tau PET and amyloid SUVR in the DS adults is driven by the difference between amyloid negative versus positive subjects rather than by amyloid SUVR, given that amyloid burden plateaus as disease progresses.

The correlation between tau burden and various cognitive and functional endpoints was striking. Although longitudinal clinical endpoints had high variability, it was notable that the highest (least affected) cognitive scores correlated with less tau burden. The longitudinal stability of CV1 suggests that this pattern is related to DS, while the

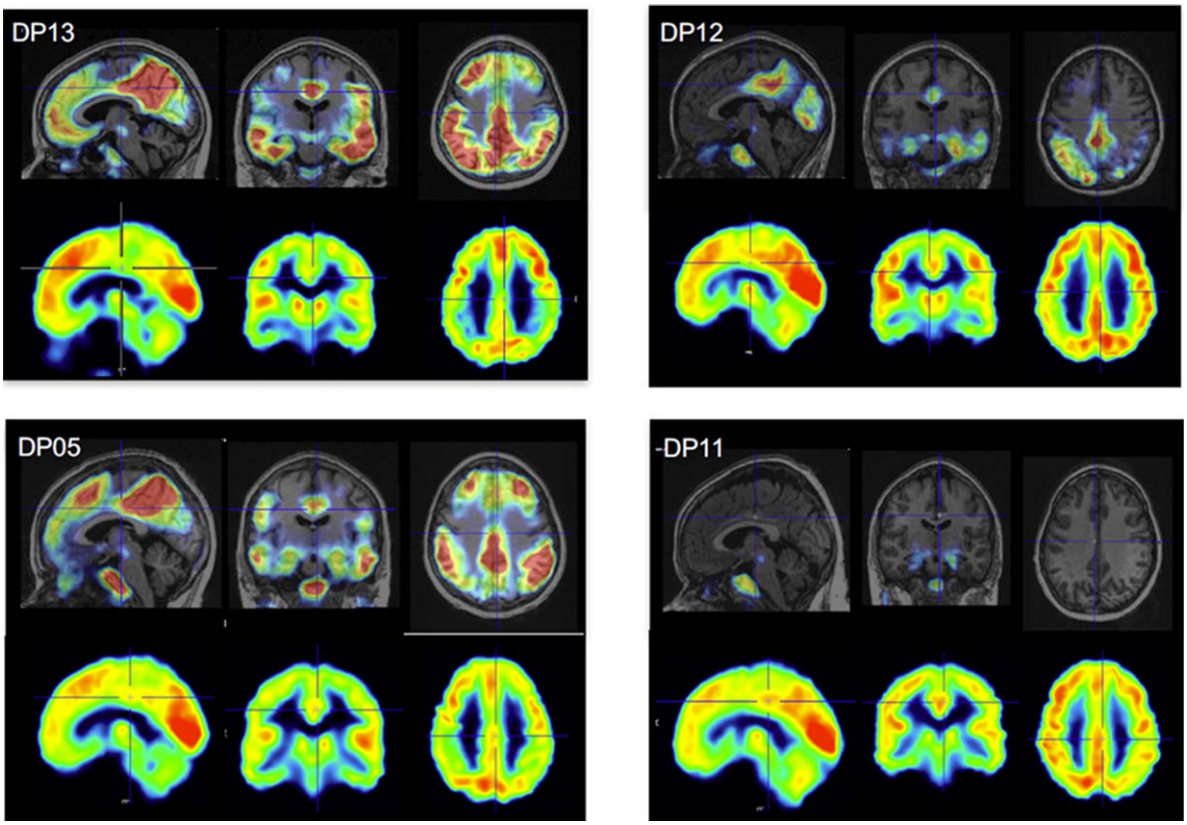

Fig. 6. Tau PET distributions (upper rows) and FDG PET images (lower rows) for four example amyloid positive subjects. In general, hypometabolism in FDG (light yellow/green rather than red) is consistent with the tau accumulation shown in red. This includes posterior cingulate and precuneus hypometabolism in subjects DP05 and DP13, and asymmetrical deposition and hypometabolism seen in subject DP12 parietal cortex and DP13 frontal cortex. However, even when tau is limited to early stages, subjects have hypometabolism as seen in DP11, which arises partially from Down syndrome and is dissociated from the effects of AD by the machine learning classifiers in this work.

AD-related CV2 pattern progresses in association with AD pathology. The lack of CV2 progression in the Am+ subject with Stage II tau is consistent with literature suggesting that neurodegeneration occurs primarily after this stage [2].

Reference region is an important consideration as evidenced in one subject. Cerebellar cortex has been applied here and in other studies [14, 30] due to its typical lack of tau in AD. However, in addition to possible tau accumulation, its location near the edge of the scanner field of view, inferior slice position relative to target regions, and low signal can make it vulnerable to technical noise as well as signal spillover, confounding measurements. White matter has been proposed as an alternate reference [32] for reasons similar to those for longitudinal amyloid measurement [33, 34]. Although tau aggregates in white matter of AD patients, levels are significantly less than in gray matter [35, 36].

A limitation to this pilot study was the small sample size. For MRI analyses, the NPAIRS software aided in addressing this through its segregation of signal from noise and prevention of model over-fitting through iterative resampling. The 2-year gap between tau PET and the amyloid and FDG PET scans was also a limitation. However, tau distributions, association with amyloid positivity and neurodegenerative status, and AD-related atrophy were striking in their consistency with findings in AD populations. Despite subject motion related noise in some scans, the robust AD-related pattern of atrophy that exhibited longitudinal progression in Am+ tau positive subjects was dissociable from that associated with DS, which was quite stable over the two years. Study of a larger cohort of subjects spanning ages 20 through 60 s could provide important additional insight.

This study and its findings are considered exploratory due to the small sample size. However,

the data shows clear trends suggesting that evaluation of therapeutic candidates for preclinical and prodromal AD has the potential to be conducted in the adult DS population, utilizing imaging biomarkers of AD pathology and neurodegeneration. When further validated using a larger study population, this could have tremendous benefit to the DS population and to the broader AD population so greatly in need of effective disease intervention.

ACKNOWLEDGMENTS

Data used in the preparation of this article were obtained from the Down Syndrome Biomarker Initiative (DSBI), the Alzheimer's Disease Neuroimaging Initiative (ADNI) database (http://adni.loni.usc.edu), and New York University.

We acknowledge and thank Janssen Research and Development for their support of the study data acquisition, the ADCS for their role in the original image data QC, Craig Pennington of ADM Diagnostics for his instrumental role in the project collaboration, Avid Radiopharmaceuticals for ^{18}F-AV-1451 Tau PET tracer, and the Alzheimer's Disease Neuroimaging Initiative and New York University for data used in comparison analyses. We also thank Mark E. Schmidt for his review of the manuscript. The development of the AD Progression Classifier by ADM Diagnostics was funded in part by SBIR grant award IIP-1256638 from the National Science Foundation.

Data collection and sharing for the ADNI comparator subjects used in this project was funded by the Alzheimer's Disease Neuroimaging Initiative (ADNI) (National Institutes of Health Grant U01 AG024904) and DOD ADNI (Department of Defense award number W81XWH-12-2-0012). ADNI is funded by the National Institute on Aging, the National Institute of Biomedical Imaging and Bioengineering, and through generous contributions from the following: AbbVie, Alzheimer's Association; Alzheimer's Drug Discovery Foundation; Araclon Biotech; BioClinica, Inc.; Biogen; Bristol-Myers Squibb Company; CereSpir, Inc.; Eisai Inc.; Elan Pharmaceuticals, Inc.; Eli Lilly and Company; EuroImmun; F. Hoffmann-La Roche Ltd and its affiliated company Genentech, Inc.; Fujirebio; GE Healthcare; IXICO Ltd.; Janssen Alzheimer Immunotherapy Research & Development, LLC.; Johnson & Johnson Pharmaceutical Research & Development LLC.; Lumosity; Lundbeck; Merck & Co., Inc.; Meso Scale Diagnostics, LLC.; NeuroRx Research; Neurotrack Technologies; Novartis Pharmaceuticals Corporation; Pfizer Inc.; Piramal Imaging; Servier; Takeda Pharmaceutical Company; and Transition Therapeutics. The Canadian Institutes of Health Research is providing funds to support ADNI clinical sites in Canada. Private sector contributions are facilitated by the Foundation for the National Institutes of Health (http://www.fnih.org). The grantee organization is the Northern California Institute for Research and Education, and the study has been coordinated by the Alzheimer's Therapeutic Research Institute. ADNI data are disseminated by the Laboratory for Neuro Imaging at the University of Southern California.

Authors' disclosures available online (http://j-alz.com/manuscript-disclosures/17-0390r1).

REFERENCES

[1] Head E, Powell D, Gold BT, Schmitt FA (2012) Alzheimer's disease in Down syndrome. *Eur J Neurodegener Dis* **1**, 353-364.

[2] Hof PR, Bouras C, Perl DP, Sparks DL, Mehta N, Morrison JH (1995) Age-related distribution of neuropathologic changes in the cerebral cortex of patients with Down's syndrome. Quantitative regional analysis and comparison with Alzheimer's disease. *Arch Neurol* **52**, 379-391.

[3] Mann DM, Yates PO, Marcyniuk B, CR Ravindra (1986) The topography of plaques and tangles in Down's syndrome patients of different ages. *Neuropathol Appl Neurobiol* **12**, 447-457.

[4] Ness S, Rafii M, Aisen P, Krams M, Silverman W, Manji H (2012) Down's syndrome and Alzheimer's disease: Towards secondary prevention. *Nat Rev Drug Discov* **11**, 655-656.

[5] Rafii MS, Wishnek H, Brewer JB, Donohue MC, Ness S, Mobley WC, Aisen PS, Rissman RA (2015) The Down Syndrome Biomarker Initiative (DSBI) Pilot: Proof of concept for deep phenotyping of Alzheimer's disease biomarkers in Down syndrome. *Front Behav Neurosci* **9**, 239.

[6] Matthews DC, Lukic AS, Andrews RD, Marendic B, Brewer J, Rissman RA, Mosconi L, Strother SC, Wernick MN, Mobley WC, Ness S, Schmidt ME, Rafii MS (2016) Dissociation of Down syndrome and Alzheimer's disease effects with imaging. *Alzheimers Dement (N Y)* **2**, 69-81.

[7] Lowe VJ, Curran G, Fang P, Liesinger AM, Josephs KA, Parisi JE, Kantarci K, Boeve BF, Pandey MK, Bruinsma T, Knopman DS, Jones DT, Petrucelli L, Cook CN, Graff-Radford NR, Dickson DW, Petersen RC, Jack CR Jr, Murray ME (2016) An autoradiographic evaluation of AV-1451 Tau PET in dementia. *Acta Neuropathol Commun* **4**, 58.

[8] Gomez T. Toward the validation of novel tau PET tracer 18F-AV-1451 (T807) in postmortem brain tissue. Available from https://www.alz.washington.edu/NONMEMBER/FALL15/NP/GomezIsla.pdf

[9] Forman MS, Zhukareva V, Bergeron C, Chin SS, Grossman M, Clark C, Lee VM, and Trojanowski JQ (2002) Signature tau neuropathology in gray and white matter of corticobasal degeneration. *Am J Pathol* **160**, 2045-2053.

[10] Nelson LD, Siddarth P, Kepe V, Scheibel KE, Huang SC, Barrio JR, and Small GW (2011) Positron emission tomography of brain β-amyloid and τ levels in adults with Down Syndrome. *Arch Neurol* **68**, 768-774.

[11] Strother SC, Anderson J, Hansen LK, Kjems U, Kustra R, Sidtis J, Frutiger S, Muley S, Laconte S, Rottenberg D (2002) The quantitative evaluation of functional neuroimaging experiments: The NPAIRS data analysis framework. *Neuroimage* **15**, 747-771.

[12] Strother SC, Oder A, Spring R, Grady C (2010) The NPAIRS Computational Statistics Framework for Data Analysis in Neuroimaging. Proceedings of COMPSTAT pp. 111-120.

[13] Ashburner J (2007) A fast diffeomorphic image registration algorithm. *Neuroimage* **38**, 95-113.

[14] Schöll M, Lockhart SN, Schonhaut DR, O'Neil JP, Janabi M, Ossenkoppele R, Baker SL, Vogel JW, Faria J, Schwimmer HD, Rabinovici GD, Jagust WJ (2016) PET imaging of tau deposition in the aging human brain. *Neuron* **89**, 971-982.

[15] Sperling R. Anti-amyloid treatment in asymptomatic Alzheimer's disease (A4 Study). https://clinicaltrials.gov/ct2/show/NCT02008357

[16] Müller-Gärtner HW, Links JM, Prince JL, Bryan RN, McVeigh E, Leal JP, Davatzikos C, Frost JJ (1992). Measurement of radiotracer concentration in brain gray matter using positron emission tomography: MRI-based correction for partial volume effects. *J Cereb Blood Flow Metab* **12**, 571-583.

[17] Mormino EC, Kluth JT, Madison CM, Rabinovici GD, Baker SL, Miller BL, Koeppe RA, Mathis CA, Weiner MW, Jagust WJ, Alzheimer's Disease Neuroimaging Initiative (2009) Episodic memory loss is related to hippocampal-mediated beta-amyloid deposition in elderly subjects. *Brain* **132**, 1310-1323.

[18] Landau SM, Breault C, Joshi AD, Pontecorvo M, Mathis CA, Jagust WJ, Mintun MA; Alzheimer's Disease Neuroimaging Initiative (2013) Amyloid-β imaging with Pittsburgh compound B and florbetapir: Comparing radiotracers and quantification methods. *J Nuc Med* **54**, 70-77.

[19] Shaw LM, Vanderstichele H, Knapik-Czajka M, Clark CM, Aisen PS, Petersen RC, Blennow K, Soares H, Simon A, Lewczuk P, Dean R, Siemers E, Potter W, Lee VM, Trojanowski JQ, Alzheimer's Disease Neuroimaging Initiative (2009) Cerebrospinal fluid biomarker signature in Alzheimer's disease neuroimaging initiative subjects. *Ann Neurol* **65**, 403-413.

[20] Faul F, Erdfelder E, Lang AG, Buchner A (2007) G*Power 3: A flexible statistical power analysis program for the social, behavioral, and biomedical sciences. *Behav Res Methods* **39**, 175-191.

[21] Drzezga A (2009) Diagnosis of Alzhiemer's disease with [18F]PET in mild and asymptomatic stages. *Behav Neurol* **21**,101-115.

[22] Mosconi L, Tsui WH, De Santi S, Li J, Rusinek H, Convit A, Li Y, Boppana M, de Leon MJ (2005) Reduced hippocampal metabolism in MCI and AD: Automated FDG-PET image analysis. *Neurology* **64**, 1860-1867.

[23] Johnson KA, Schultz A, Betensky RA, Becker JA, Sepulcre J, Rentz D, Mormino E, Chhatwal J, Amariglio R, Papp K, Marshall G, Albers M, Mauro S, Pepin L, Alverio J, Judge K, Philiossaint M, Shoup T, Yokell D, Dickerson B, Gomez-Isla T, Hyman B, Vasdev N, Sperling R (2016) Tau positron emission tomographic imaging in aging and early Alzheimer disease. *Ann Neurol* **79**, 110-119.

[24] Gonzalez LM, Anderson VA, Wood SJ, Mitchell LA, Heinrich L, Harvey AS (2008) The Observer Memory Questionnaire-Parent Form: Introducing a new measure of everyday memory for children. *J Int Neuropsychol Soc* **14**, 337-342.

[25] F. Carducci F, Onorati P, Condoluci C, De Gennaro G, Quarato PP, Pierallini A, Sará M, Miano S, Cornia R, Albertini G (2013) Whole-brain voxel-based morphmetry study of children and adolescents with Down syndrome. *Funct Neurol* **28**, 19-28.

[26] Smigielska-Kuzia J, Boćkowski L, Sobaniec W, Sendrowski K, Olchowik B, Cholewa M, Lukasiewicz A, Lebkowska U (2011) A volumetric magnetic resonance imaging study of brain structures in children with Down syndrome. *Neurol Neurochir Pol* **45**, 363-369.

[27] Thompson PM, Mega MS, Woods RP, Zoumalan CI, Lindshield CJ, Blanton RE, Moussai J, Holmes CJ, Cummings JL, Toga AW (2001) Cortical change in Alzheimer's disease detected with a disease-specific population-based brain atlas. *Cereb Cortex* **11**, 1-16.

[28] Dukart J, Mueller K, Villringer A, Kherif F, Draganski B, Frackowiak R, Schroeter ML, Alzheimer's Disease Neuroimaging Initiative (2013) Relationship between imaging biomarkers, age, progression and symptom severity in Alzheimer's disease. *Neuroimage Clin* **3**, 84-94.

[29] Ossenkoppele R, Schonhaut DR, Schöll M, Lockhart SN, Ayakta N, Baker SL, O'Neil JP, Janabi M, Lazaris A, Cantwell A, Vogel J, Santos M, Miller ZA, Bettcher BM, Vossel KA, Kramer JH, Gorno-Tempini ML, Miller BL, Jagust WJ, Rabinovici GD (2016) Tau PET patterns mirror clinical and neuroanatomical variability in Alzheimer's disease. *Brain* **139**, 1551-1567.

[30] Schwarz AJ, Shcherbinin S, Miller BB, Yu P, Navitsky M, Dickson J, Joshi AD, Devous MD Sr, Mintun MA (2015) Hippocampal sparing and limbic predominant tau subtypes of Alzheimer's disease determined *in vivo* using [18F]-AV-1451 PET imaging. *Alzheimers Dement* **11**, P144-P145.

[31] Sepulveda-Falla D, Matschke J, Bernreuther C, Hagel C, Puig B, Villegas A, Garcia G, Zea J, Gomez-Mancilla B, Ferrer I, Lopera F, Glatzel M (2011) Deposition of hyperphosphorylated tau in cerebellum of PS1 E280A Alzheimer's disease. *Brain Pathol* **21**, 452-463.

[32] Rogers MB (2016) Improving Tau PET: In Search of Sharper Signals: Report from AAIC http://www.alzforum.org/news/conference-coverage/improving-tau-pet-search-sharper-signals, Posted 23 August 2016.

[33] Schwarz CG, Senjem ML, Gunter JL, Tosakulwong N, Weigand SD, Kemp BJ, Spychalla AJ, Vemuri P, Petersen RC, Lowe VJ, Jack CR Jr (2017) Optimizing PiB-PET SUVR change-over-time measurement by a large-scale analysis of longitudinal reliability, plausibility, separability, and correlation with MMSE. *Neuroimage* **144**, 113-127.

[34] Chen K, Roontiva A, Thiyyagura P, Lee W, Liu X, Ayutyanont N, Protas H, Luo JL, Bauer R, Reschke C, Bandy D, Koeppe RA, Fleisher AS, Caselli RJ, Landau S, Jagust WJ, Weiner MW, Reiman EM, Alzheimer's Disease Neuroimaging Initiative (2015) Improved power for characterizing longitudinal amyloid-β PET changes and evaluating amyloid-modifying treatments with a cerebral white matter reference region. *J Nucl Med* **56**, 560-566.

[35] Mukaetova-Ladinska EB, Harrington CR, Roth M, Wischik CM (1993) Biochemical and anatomical redistribution of tau protein in Alzheimer's disease. *Am J Pathol* **143**, 565-578.

[36] Khatoon S, Grundke-Iqbal I, Iqbal K (1994) Levels of normal and abnormally phosphorylated tau in different cellular and regional compartments of Alzheimer disease and control brains. *FEBS Lett* **351**, 80-84.